International Journal of Science and Research (IJSR)
ISSN (Online): 2319-7064
Index Copernicus Value (2015): 78.96 | Impact Factor (2015): 6.391

Synthesized and Characterization of $Cr_xCu_{0.25}Zn_{0.75-x}Fe_2O_4$ Nanoparticles using Sol–Gel Auto Combustion Method

Tariq A. Al-Dhahir[1], Bassam T. Al-Azraq[2]

[1, 2] Department of physics, College of Education for Pure Science -Ibn Al-Haitham, Baghdad University, Iraq

Abstract: ***$Cr_xCu_{0.25}Zn_{0.75-x}Fe_2O4$ with (x=0.0 ,0.25, 0.35,0.45,0.55,0.65,0 and 0.75) spinal ferrite nanoparticles have been synthesized via sol – gel auto combustion method . The result powder was calcined at temperature of 850Ċ for 3 hours. Structural and electrical properties of $Cr_xCu_{0.25}Zn_{0.75-x}Fe_2O_4$ were investigated using x – ray diffraction (XRD) , scanning electron microscopy (SEM) , energy dispersive x – ray spectroscopy (EDS) and LCR meter . XRD pattern of $Cr_xCu_{0.25}Zn_{0.75-x}Fe_2O_4$ provides information about single-phase formation of spinal structure with cubic symmetry. SEM technique demonstrated that nanoparticles with grain size found to be in nanometer range. Particle size, lattice constant and porosity decrease with increasing Cr content, while bulk density. Both ε' and ε'' decrease when there is increasing in the frequency, from another side they are increasing when Cr content increased***

Keywords: Sol – Gel, $Cr_xCu_{0.25}Zn_{0.75-x}Fe_2O_4$, Structural and Dielectric Properties

1. Introduction

The prepared Nano – ferrites show a significant change in the structural, electrical and magnetic properties in contrast to their bulk counterparts due to their high surface - volume ratio of grains [1]. Ferrites constitute a special branch of ferromagnetic. In the recent years, interest in the Nano-ferrites has increasing, due to their high magnetic properties and widely employing in several applications. Ferrites are using in the electronic devices, integrated circuits and magnetic resonance imaging (MRI) [2,3]. Nano – phase spinal ferrite particles have attracted a considerable attention owing to their technological importance in the industrial applications [4]. Spinal ferrite can be represented by the chemical formula $MFe2O_4$, where M is the bivalent metal such as (Mg, Zn, Mn, Co, Cu … etc.), with radius lying between (0.6 – 1)Å and that gives stable crystal structures. Fe^{+3} indicates to the trivalent iron cation. The unit cell of spinal ferrite has a symmetry of 8 structural formulas with O^{-2} anions which lead to form a face-centered cubic among O^{-2} anions. Cations distributed in two groups of sites are A and B, A - sites, cation surrounded by (4) neighboring oxygen anions, A - sites called tetrahedral - sites, While in B - sites, the cation surrounded by 6 oxygen anions, called octahedral – sites[5,6]. There is no previous literature of Cr substitution Zn ferrite, anyway, there are a similar studies of Cr effects on the structural, electrical and magnetic properties of a different compounds reported by [7-9]. Nano – ferrite can be prepare by many techniques; one of them is the low coast sol - gel auto combustion method, which used in this study. The sol – gel auto combustion method characterized by its easy, short time and required no high temperatures in the preparation process [10].

2. Experimental Details

$Cr_xCu_{0.25}Zn_{0.75-x}Fe_2O_4$ with (x= 0.0, 0.25, 0.35, 0.45, 0.55, 0.65 and 0.75) have been synthesized by sol – gel auto combustion method. The hydrated nitrates Fe $(NO_3)_3$. $9H_2O$, Cr $(NO_3)_3$. $9H_2O$, Cu $(NO3)_2$. $2H_2O$ and Zn $(NO_3)_2$. $6H_2O$ were used as a precursor materials dissolved in 100 mL of distilled water. Hydrated citric acid ($C_6H_8O_7$) was used as a fuel of chemical reaction dissolved in 100 mL of distilled water with molar ratio of these nitrates and citric acid becomes 1:0.5. Drops of ammonia was added to set (PH) about of (7). The solution was stirred using magnetic stirrer. Condensation reaction occurs between the adjacent metal nitrates and the molecules of citrates to get a sol at room temperature. Solution was evaporated at 80Ċ for 1h with continuous stirring until the sol turned into a gel. The gel was then hated at 180Ċ for auto combustion to take place . The dried gel was burnt spontaneously to form as a powder. The resulting powder was crushed using an agate mortar to obtain the Nano-ferrite. The Nano – powder was calcined at 850Ċ for 3h. 2.5 g of the powder was pressed using a hydraulic pressing with (1 ton) applied pressure for 3 min. Stainless steel mold with 1.5 cm diameter was used to preparing pellets. Pellets were sintered initially at 900Ċ and finally at 1200Ċ both final and initial sintering for 3h.

3. Results and Discussion

The title of the paper is centered 17.8 mm (0.67") below the top of the page in 24 point font. Right below the title (separated by single line spacing) are the names of the authors. The font size for the authors is 11pt. Author affiliations shall be in 9 pt.

3.1 X-ray diffraction analysis

The x – ray diffraction pattern of the Cr Cu Zn ferrite with (x= 0.0, 0.25, 0.35, 0.45, 0.55, 0.65 and 0.75) are explained in figure (1). XRD technique provided information about formation of single-phase cubic spinal structure. All the Bragg's peaks of XRD pattern are broad and do not contain any extra peaks other than the cubic spinal phase, as reported in the literature [11].

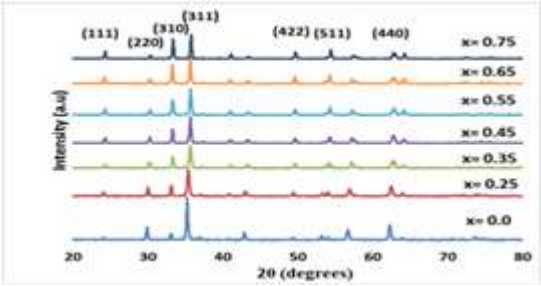

Figure 1: The XRD pattern of $Cr_xCu_{0.25}Zn_{0.75-x}Fe_2O_4$ samples

3.1.1 Particle size

Particle size was calculated using Debye – sherrer formula [12]:

$$D = \frac{0.89\,\lambda}{\beta cos\theta} \quad (1)$$

Where D is the particle size, 0.9 is the symmetry constant, λ is the wavelength of incident x – ray beam and θ is Bragg's angle. The calculated particle sizes are in the range of 27 – 32 nm and exhibit gradual decrease with increasing Cr^{+3} .

3.1.2 The lattice constant

The lattice constant (a) for each sample is calculated by the following relationship [13]:

$$d_{hkl} = \frac{a}{\sqrt{h^2+k^2+l^2}} \quad (2)$$

Where d_{hkl} is the interplanar distance for hkl planes, Lattice constant was found to decrease with increasing of Cr content from (8.41 Å) to (8.2835 Å). The decrement of particle size and lattice constant due to the ionic radius of Cr (0.63 Å), which is smaller than of Zn (0.83 Å) as reported in the literature [14,15].

3.1.3 X – Ray and bulk densities

The x-ray density $\rho_{x\text{-}ray}$ of the synthesized samples was calculated using next formula [16]:

$$\rho_{x-ray} = \frac{8M}{Na^3} \quad (3)$$

Where M is the molecular weight of the composition, a is the lattice constant and N is the Avogadro's number ($6.02*10^{23}$atom/mole). Bulk density (ρ_b) of the prepared samples was measured using the following equation:

$$\rho_b = \frac{m}{V} \quad (4)$$

Where m is the mass of pellets and V is the volume of pellet which was measured using Archimedes principle ; Both $\rho_{x\text{-}ray}$ and ρ_b increase with increasing Cr content due to the difference in the ionic radii which leads to decreasing pellet volume of the sample. $\rho_{x\text{-}ray}$ in the table (1) is larger than ρ_b that's may be due to the presence of some unavoidable voids during sintering, the same results are reported by [17,18].

3.1.4 Porosity

Porosity of each sample was found to decrease with increasing Cr content according to the following formula [19]:

$$P = \left[1 - \frac{\rho_b}{\rho_{x-ray}}\right] * 100\% \quad (5)$$

Where ρ_b , $\rho_{x\text{-}ray}$ are the bulk and x – ray densities respectively. The decrement in the porosity due to decreasing particle size.

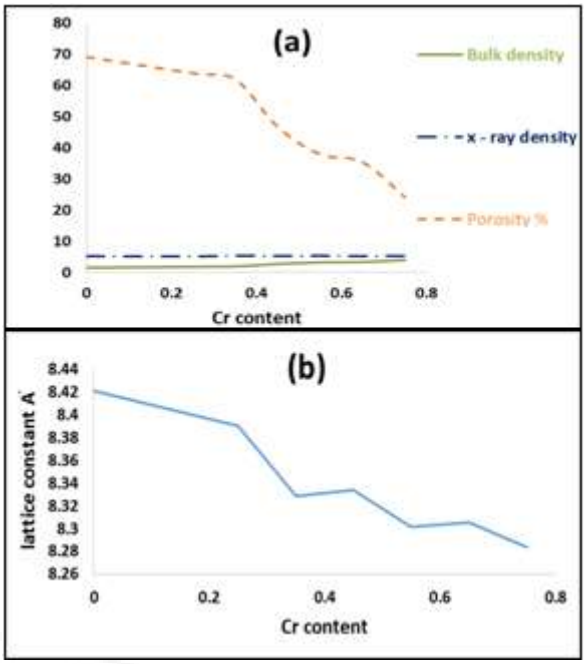

Figure 2: (a) The change of porosity, x – ray density and bulk densities with Cr content. (b) The change in lattice constant with varying Cr content.

Table 1: The values of lattice constant, x – ray density, bulk density and particle size versus Cr concentration.

Sample	Lattice constant (Å)	*X – ray density* ρ_{x-ray} *(g/cm^3)*	*Bulk density* ρ_b *(g/cm^3)*	*Porosity P (%)*	*Particle size D (nm)*
A1	8.41	5.351	1.654	69	32
A2	8.39	5.335	1.927	63.8	30.2
A3	8.32836	5.424	2.0625	61.97	29
A4	8.334	5.382	2.8638	46.789	28.42
A5	8.3016	5.414	3.354	38	27.63
A6	8.305	5.376	3.4664	35.52	27.2
A7	8.2835	5.387	4.075	24.355	31

3.2 Scanning electron microscopy (SEM) analysis

Surface morphological properties of $Cr_{0.75}Cu_{0.25}Fe_2O_4$ were studied using scanning electron microscopy (SEM). Figure (2) shows that SEM micrograph of $Cr_{0.75}Cu_{0.25}Fe_2O_4$ (A7) sample, this micrograph reveals that the distribution of particle size is uniformed and the particle size in the nanometer range, which is about of 36 nm for (A7) sample.

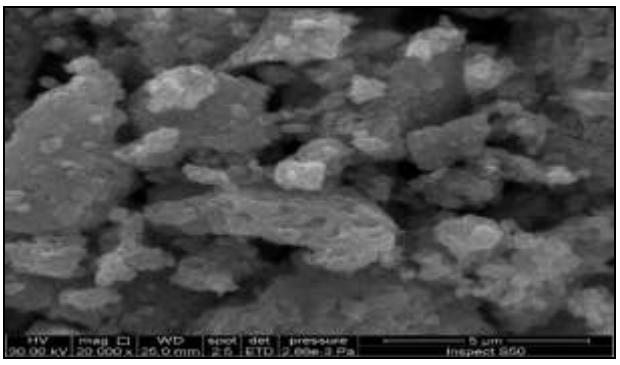

Figure 3: SEM morphology of $Cr_{0.75}Cu_{0.25}Fe_2O_4$ powder

3.3 Energy dispersive x - ray spectroscopy

The elemental analysis of (A7) sample has been carried out using (EDS). It revealed from figure (3) that the concentration of iron, chromium and copper is according to the stoichiometric calculations.

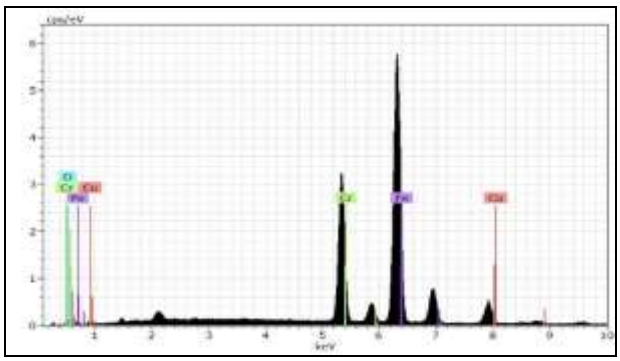

Figure 4: Elemental analysis of $Cr_{0.75}Cu_{0.25}Fe_2O_4$ powder using EDS technique

3.4 Dielectric properties of the prepared samples

Dielectric properties of the synthesized samples were studied using LCR meter, both dielectric constant Ɛ' and dielectric loss factor Ɛ" were calculated using the equations 5,6 respectively. These dielectric properties were measured as a function with frequency at room temperature. At low frequency (less than 5 kHz), Ɛ' and Ɛ" began with a high value then decrease gradually with increasing frequency. This decrement can discussed by mechanisms of polarization. There are four mechanisms of polarization are space charge, atomic / ionic, electronic and orientational polarization. The space charge dipoles have a high mass , so at high frequency (above 5kHz) these dipoles could not rotate with the external A.C electrical field , then these dipoles don't take a part of polarization , therefore the value of Ɛ' and Ɛ" decrease gradually with increasing frequency. Figure (5 – a,b) explaining the decrement in Ɛ', Ɛ" with frequency (5 kHz – 1MHz). In the other side, both Ɛ' and Ɛ" increase with increasing Cr content as in figure (5 – c,d) due to the increase of the number of charge carriers and interfacial polarization effects, as reported by [20].

$$\varepsilon' = \frac{Cd}{\epsilon_0 A} \qquad (6)$$

Where ε' is the dielectric constant, C the capacitance (Farad), d thickness of the sample, A surface area of the sample and ϵ_0 is permittivity and equal to $8.85*10^{-12}$ $N.m^2/C^2$ [21].

$$\varepsilon'' = \varepsilon' \tan \delta \qquad (6)$$

Where ε'' is the dielectric loss fctor and $\tan \delta$ is the dissipation factor [22].

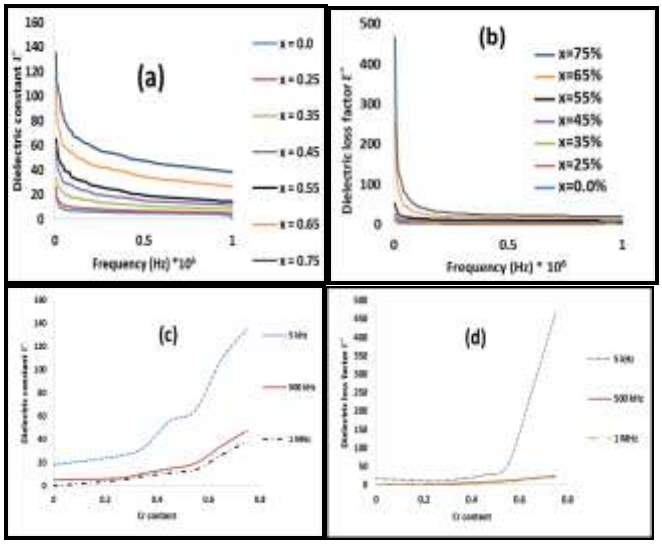

Figure 5: (a) And (b) represent the decrement in the dielectric constant and dielectric loss factor respectively when the frequency increased. (c) and (d) show the increment in the dielectric constant and dielectric loss factor respectively with increasing Cr content.

4. Conclusions

Cr substituted Zn into $Cr_xCu_{0.25}Zn_{0.75-x}Fe_2O_4$ with (x= 0.0, 0.25, 0.35, 0.45, 0.55, 0.65 and 0.75) were prepared using sol – gel auto combustion method. The structural characterization of powder using XRD, SEM and EDS confirmed the formation of nanosize particles with single-phase spinal structure. Particle size and lattice constant decrease when Cr concentration increased that's due to the ionic radius of Cr^{+3} smaller than of Zn. Both bulk and x – ray densities increase with increasing Cr content. Porosity decreases when Cr content increased this is due to the decrement in the particle size. Both dielectric constant and dielectric loss factor decrease when the frequency increased, whereas they increase with increasing Cr content.

References

[1] Iqbal, M. J., Ahmed, Z., Meydan, T., Melikhov, Y.: Physical, electrical and magnetic properties of nano – sizes Co – Cr substituted magnesium ferrites. J. Appl. Phys. 111, 033906 (2012).
[2] Kumar, A.M., Varma, M.C., Dube, C.L., Rao, K., Kashyap, S.C.: Development of Ni – Zn nanoferrite core material with improved saturation magnetization and DC resistivity. J. Magn. Magn. Mater.320, 1995 – 2000 (2008).
[3] Ritu Rain, Gagan Kumar, Khalid Mujasam Batoo, M. Singh: Electrical and Dielectric of Zinc Substituted Cobalt Nanoferrites Prepared by Solution Combustion Method. American Journal of Nanomaterials, 19 – 12 (2013).
[4] V.V.AWATI: Synthesis and Characterization of Ni-Cu-Zn Ferrite Materials by Auto Combustion Technique. International Journal of Chemical and Physical Science, 4, 50 – 59 (2015)
[5] F.S. Tehrani, " Structural, magnetic, and optical properties of zinc- and copper substituted nickel ferrite

nanocrystals", MSc, Alzhara University,Tehran , Iran,1-8,(2012).

[6] Rapolu Sridhar, Dachepalli Ravinder, K. Vijaya Kumar: Synthesis and Characterization of Copper Substituted Nickel Nano-Ferrites by Citrate-Gel Technique. Advance in materials Physics and Chemistry, 2, 192 – 199 (2012).

[7] M. Lakshmi.: An investigation of structural and magnetic properties of Cr – Zn ferrite nanoparticles prepared by a sol-gel process. J Nanostruct Chem. 5(4), 365-373 (2015)

[8] S. J. Lee and C. C. H. Lo,: Magnetic and magnetoelastic properties of Cr – substituted cobalt ferrite. Journal of Applied Physics, 102, 073910, (2007)

[9] A. M. El-Sayed,: Electrical conductivity of nickel-zinc and Cr substituted nickel – zinc ferrite. Materials Chemistry and Physics, 82, 583-587 (2003).

[10] Ramkrishna H Kadam.: Infiuence of Cr^{+3} substitution on the electrical and magnetic properties of $Ni_{0.4}Cu_{0.4}Fe_2O_4$ nanoparticles. International Nano Letters. 2:28 (2012)

[11] Andris SUTKA and Gundars MEZINSKIS: Sol – gel auto-combustion synthesis of spinal – type ferrite nanomaterials. Front. Mater. Sci. 6 (2), 128 – 141 (2012).

[12] Asmaa A . H. EL – Bassuony: Enhancement of structural and electrical properties of novelty nanoferrite materials. J Mater Sci: Mater Electron, DOI 10. 1007/s1085-017-7312-9 (2017).

[13] K. Rajasekhar Babu . K. Rama Rao . B. Rajesh Babu: Effect of Cu and Cation Redistribution on Structural and Magnetic Properties of Co-Mg Nanoferrite. J Supercond Nov Magn, DOI 10. 1007/s10948-017-4068-7 (2017).

[14] Ram Kripal Shamrma . Omprakash Suwalka. N. Lakshmi . K. Venugopalan: Mossbauer studies of Cr substituted bulk and nam Co-Zn ferrites. Hyperfine Interact, 165, 261 – 266 (2005).

[15] T. Pandiyarajan. B. Karthikeyan: Cr doping induced structural, phonon and excitonic properties of ZnO nanoparticles. J Nanopar Res, 14, 647 – 656 (2012).

[16] Davuluri Venkatesh. G. Himavathi. K. V. Ramesh: Structural, Magnetic, and Electrical Properties of $Ni_{0.65}Zn_{0.35-x}Cu_xFe_2O_4$ Nanoferrite System. J Supercond Nov Magn, DOI 10. 1007/s10948-0

[17] Muhammad Javad Iqbal , Zahoor Ahmed, Yevgen Melikhov , Ikenna Cajetan Nlebedim: Effect of Cu-Cr co-substitution on magnetic properties of nanocrystalline magnesium ferrite. Journal of Magnetic Materials, 324, 1088 – 1094 (2012).

[18] S. R. Bainade . C. M. Kale . M. C. Sable: Effect Cr^{+3} Ions Substitution on Structural and Magnetic Properties of Co Ferrite Nanoparticles. J Supercond Nov Magn, DOI 10.1007/s 10948-017-4205-3.

[19] K. M. Batoo: Low temperature-fired Ni-Cu-Zn ferrite nanoparticles through auto-combustion method for multilayer chip inductor applications. J Springer, 7(112), 1-14, (2012).

[20] S. A. Gad. A. M. Moustafa. A. A. Ward: Preparation and some physical properties of $Zn_{1-x}Cr_xO$. J Inorg Organomet Polym, 25(5), 1077 – 1087 (2015)

[21] C.J. Mathai, S. Saravanan, M. R.Anantharaman, S. Venkitachalam, and S. Jayalekshmi.: Characterization of low dielectric constant polyaniline thin film synthesized by ac plasma polymerization technique. Journal of physics D. Applied physics. 35 (3) . 240 – 245 (2002)